Inhalable chitosan microparticles for simultaneous delivery of isoniazid and rifabutin in lung tuberculosis treatment

Ludmylla Cunha[a,b], Susana Rodrigues[a,b], Ana M. Rosa da Costa[c,d], Leonor Faleiro[a] Francesca Buttini[e], and Ana Grenha[a,b,d]*

[a]*Centre for Biomedical Research, University of Algarve, 8005-139, Faro, Portugal; a49277@ualg.pt (L.C.); susananasus@gmail.com (S.R.); mfaleiro@ualg.pt (M.L.F.);* [b]*Centre for Marine Sciences, University of Algarve, 8005-139, Faro, Portugal;* [c]*Algarve Chemistry Research Centre, University of Algarve, 8005-139, Faro, Portugal; amcosta@ualg.pt;* [d]*Department of Chemistry and Pharmacy, Faculty of Sciences and Technology, University of Algarve, 8005-139, Faro, Portugal* [e]*Food and Drug Department, University of Parma, 43124 Parma, Italy; francesca.buttini@unipr.it*

*corresponding author: amgrenha@ualg.pt; Tel.: +351-289-244-441; Fax: +351-289-800-066.

Abstract

The direct delivery of antibiotics to the lung has been considered an effective approach to treat pulmonary tuberculosis, which represents approximately 80% of total cases. In this sense, this work aimed at producing inhalable chitosan microparticles simultaneously associating isoniazid and rifabutin, for an application in pulmonary tuberculosis therapy. Spray-dried chitosan microparticles were obtained with adequate flow properties for deep lung delivery (aerodynamic diameter of 4 μm) and high drug association efficiencies (93% for isoniazid and 99% for rifabutin). The highest concentration of microparticles that was tested (1 mg/mL) decreased the viability of macrophage-differentiated THP-1 cells to around 60% after 24 h exposure, although no deleterious effect was observed in human alveolar epithelial (A549) cells. The release of LDH was, however, increased in both cells. Chitosan microparticles further evidenced capacity to activate macrophage-like cells, inducing cytokine secretion well above basal levels. Moreover, the propensity of macrophages to internalise microparticles was demonstrated, with uptake levels over 90%. Chitosan microparticles also inhibited bacterial growth by 96%, demonstrating that the microencapsulation preserved drug antibacterial activity *in vitro*. Overall, the obtained data suggest the potential of chitosan microparticles systems for inhalable lung tuberculosis therapy.

Keywords: chitosan, inhalable microparticles, isoniazid, rifabutin, spray-drying, pulmonary tuberculosis.

1. Introduction

Although tuberculosis (TB) is a curable condition, in 2016 it caused 1.3 million deaths worldwide [1]. As pulmonary TB represents approximately 80% of total cases, the

direct delivery of antibiotics to the infection site has been explored as an effective approach to treat the disease. However, the airway structure, local degradation and specific defence mechanisms (e,g. mucociliary clearance) are some limitations imposed by the pulmonary route [2]. Such limitations may be overcome by drug microencapsulation, a strategy that demands the design of inhalable carriers capable of reaching the alveoli, where infected macrophages reside. Additionally, further benefit may be attained if the carriers can be recognised by macrophage surface receptors. This can be mediated by the chemical composition of chitosan (CS), composed by *N*-acetylglucosamine and D-glucosamine residues, the former already described to be recognised by macrophages [3], thus, possibly, potentiating phagocytosis. Other materials have been proposed to mediate the referred macrophage recognition and our group has recently published other works reporting the ability of fucoidan microparticles to provide this effect [4,5]. Nevertheless, CS is, in comparison, much more explored as matrix material, while the report of macrophage targeting ability of CS-based microparticles is scarce. In turn, CS microparticles were previously proposed as inhalable carriers of isoniazid [6], in a study focusing essentially on the chemical analysis of microparticles and their mucoadhesive capacity.

In this context, the present work aimed at producing inhalable CS microparticles (MP) that efficiently associate both isoniazid (INH) and rifabutin (RFB) in a single formulation for an application in pulmonary TB therapy. The proposed combined therapy is in agreement with WHO guidelines recommended for active pulmonary TB [1]. Microparticles were characterised and their respirability evaluated along with biocompatibility and antibacterial activity *in vitro*. Furthermore, the potential affinity of the produced carriers for alveolar macrophages was assessed, as well as their capacity to activate the target cells.

2. Materials and methods

2.1. Materials

CS (low molecular weight, 75-85% deacetylation degree, 116 *k*Da), buffer solution pH 5 (citric acid ~0.096 M, sodium hydroxide ~0.20 M), dimethylformamide (DMF), Dulbecco's modified Eagle's medium (DMEM), hydrogen chloride (HCl), isoniazid (INH,), lipopolysaccharide (LPS), *N*-(3- dimethylaminopropyl)-*N′*-ethylcarbodiimide hydrochloride (EDAC), non-essential amino acids solution, penicillin/streptomycin (10000 units/mL, 10000 g/mL), sodium dodecyl sulphate (SDS), trypan blue solution (0.4%), trypsin-EDTA solution (2.5 g/L trypsin, 0.5 g/L EDTA), and triton-X 100 were purchased from Sigma-Aldrich (Germany). Lactate dehydrogenase (LDH) kit was supplied by Takara Bio (Tokyo, Japan), while RPMI 1640 and Ham's F12 media were provided by Lonza Group AG (Switzerland). Rifabutin (RFB) was obtained from Chemos (GmbH, Germany) and phorbol 12-myristate 13-acetate (PMA) by Cayman Chemicals (USA). Tween 80®, Phosphate buffer saline (PBS) tablets pH 7.4, and thiazolyl blue tetrazolium bromide (MTT) were purchased from Amresco (USA). Dimethyl sulfoxide (DMSO) was supplied by VWR (France) and fetal bovine serum (FBS) along with L-glutamine solution (200 mM) by Gibco (Life Technologies, USA). Middlebrook 7H9 (M7H9; 4.7 g/L) and OADC (oleic acid, albumin, dextrose and catalase) were obtained from Remel (Lenexa, USA). Quantikine® HS ELISA kits for TNF-α and IL-8 were from R&D Systems (USA). All other chemicals were reagent grade. Ultrapure water (MilliQ, Millipore, UK) was used throughout the studies.

2.2 Microparticle production

Microparticles were obtained from CS (2% w/v, dissolved in 1% v/v acetic acid) solutions, containing both INH and RFB. INH was solubilised in 1% (v/v) acetic acid,

whereas RFB was dissolved in 10% (v/v) ethanol. Drugs were ground prior to solubilisation and afterwards incorporated dropwise into the CS solution. Drugs were added to obtain final CS/INH/RFB mass ratio of 10/1/0.5. A formulation of CS/INH/RFB = 10/1/0.2 (w/w) was specifically produced to be used in cytotoxicity assays (Section 2.8). CS solutions (with and without drugs) were spray-dried, using a spray-dryer (Büchi B-290 Mini Spray Dryer, Switzerland) equipped with a high-performance cyclone, and operated as follows: spray flow rate of 473 L/h, aspirator at 80%, inlet temperature of 160 ± 1 ºC and feed flow of 1.3 mL/min. The production yield was calculated as a percentage of the total solid content in the feed dispersion.

Fluorescent CS microparticles were also produced to be used in a single assay (macrophage capture – section 2.8). Briefly, CS (1% w/v, dissolved in 0.1 M acetic acid) reacted with fluorescein in the presence of EDAC [7]. After stirring (24 h, protected from light), the reaction mixture was dialysed against distilled water. The resulting solution was frozen, freeze-dried (FreeZone Benchtop Freeze Dry System, USA) and finally spray-dried, as described above, to produce unloaded fluorescent microparticles.

2.3. Surface morphology and particle size

The morphology of CS microparticles was observed with field emission scanning electron microscopy (FESEM Ultra Plus, Zeiss, Germany). To do so, samples were placed onto metal plates and sputter-coated (model Q150T S/E/ES, Quorum Technologies, UK) with iridium (5 nm thick).

The median volume diameter ($D_{(v,0.5)}$) was determined using a SprayTec® (Malvern, UK), after dispersing microparticles (15 mg) in 2-propanol (15 mL) and sonicating (5 min). Analyses (n = 3) were performed with an obscuration threshold of 10% [8].

2.4. Drug association efficiency and loading capacity

Drug content was determined by dissolving dry powder (30 mg) in HCl 0.1 M (10 mL), under constant stirring (20 min). Then, the solution was filtered (cellulose acetate, 0.45 µm) before quantification by UV-Vis spectrophotometry (Pharmaspec UV-1700, Shimadazu, Japan) at 268.5 nm (INH) and 500 nm (RFB). The measurement at 500 nm provided a direct calculation of the RFB amount present in CS microparticles. In turn, the measurement performed at 268.5 nm required a 1:10 dilution and represented the sum of amounts of INH and RFB. The amount of INH was thus calculated by subtracting the amount of RFB from this value. Calibration curves were obtained from standard solutions of both drugs prepared using the medium resulting from dissolution of unloaded microparticles in HCl 0.1M. Drug association efficiency (AE) and microparticle loading capacity (LC) were estimated (n = 3) as follows [6]:

$$AE\ (\%) = (\text{Real amount of drug} / \text{Theoretical drug content}) \times 100 \quad (1)$$

$$LC\ (\%) = (\text{Real drug content} / \text{Weight of microparticles}) \times 100 \quad (2)$$

2.5. In vitro aerosolisation

The aerodynamic assessment was determined as previously described in the literature [9], using the Andersen cascade impactor (ACI, Copley Scientific Ltd., UK) at a flow rate of 60 L/min. Cut-offs of the stages from −1 to 6 are the following: 8.60, 6.50, 4.40, 3.20, 1.90, 1.20, 0.55 and 0.26 µm. For each determination (n = 3), three capsules (HPMC size 3; Quali-V-I, Qualicaps, Spain) were manually filled with microparticles (30 mg/capsule) and aerosolised using the RS01 dry powder inhaler (Plastiape Spa, Italy). Aerosolised microparticles were rinsed with a mixture of water/acetonitrile (50/50, v/v), then sonicated (5 min), and filtered (0.45 µm, RC, Sartorius, USA). Drug deposition on

each stage of the ACI was determined by HPLC (Agilent 1200 series, Germany) at 275 nm (diode array detector). The mobile phase was phosphate buffer 20 mM pH = 7 (A) and acetonitrile (B). The gradient started with 95:5 (A:B) during 5 min, reaching a ratio of 30:70 (A:B), in the following 3 min, a condition kept for 19 min. The injection volume was 20 µL and the flow rate was set at 1 mL/min. Drug deposition on each stage was determined from standard calibration curves.

2.6. Drug release

In vitro drug release was conducted in citrate buffer pH 5 and PBS pH 7.4, both containing 1% (v/v) Tween® 80. To do so, dry powder (15 mg) was suspended in the release medium (10 mL) and maintained under mild shaking (100 rpm; Orbital Shaker OS 10, Biosan, Latvia) at 37 ºC (Dry line; VWR, USA). Samples of 1 mL were taken at pre-established time intervals, centrifuged (16,000 *x g*, 15 min; Heraeus Fresco 17 Centrifuge, ThermoScientific, USA) and then filtered (0.45 µm). Drug quantification was performed by spectrophotometry as described above (section 2.5). Calibration curves were established using standard solutions of drugs dissolved in the medium resulting from the incubation of unloaded CS microparticles with the release medium, followed by centrifugation (4000 rpm, 20 min; Centrifuge MPW 223e, Poland) and filtration (0.45 µm).

2.7. Evaluation of cytotoxicity

The cytotoxic profile of microparticles was evaluated by the MTT assays and the LDH release assay. A549 cells (American Type Culture Collection, UK) and THP-1 human monocytic cells (Leibniz-Institut DSMZ, Germany) were used, the latter

undergoing a pre-treatment with PMA (50 nM, 48 h exposure) for differentiation into macrophage phenotype [10].

To perform the assays, A549 cells (1.0 x 10^4 cells/well) and macrophage-differentiated THP-1 cells (3.5 x 10^5 cells/well) were exposed (3 h and 24 h) to unloaded and drug-loaded CS microparticles at concentrations of 0.1, 0.5 and 1.0 mg/mL. Dry powders were dispersed in the proper cell culture medium (CCM) without FBS. Free drugs were tested as control at concentrations equivalent to their theoretical loadings in microparticles: 0.01, 0.05 and 0.1 mg/mL (INH) and 0.005, 0.025 and 0.05 mg/mL (RFB). SDS (solution at 2%, w/v) was used as negative control of cell viability. The viability of treated cells was expressed as a percentage of that observed for the positive control (untreated cells).

In simultaneous assays, the amount of LDH released by the cells upon contact with the microparticles (1 mg/mL) and controls was measured upon 24 h. Cell supernatant was collected, centrifuged and analysed using a commercial kit. LDH was quantified by spectrophotometry at 490 nm (Infinite M200, Tecan, Austria), with background correction at 690 nm. CCM was used as negative control and Triton-X100 as positive control (100% LDH release). LDH released upon incubation with each sample was determined by comparison with the positive control. The assay was performed in triplicate.

2.8. Interaction of CS microparticles with macrophages

The ability of macrophage-like cells to internalise CS microparticles was evaluated by flow cytometry (FacScalibur cell analyser, BD Biosciences, Belgium). Macrophage-differentiated THP-1 (3.50 x 10^5 cells/mL) and rat alveolar macrophages NR8383 cells (2.0 x 10^5 cells/mL) were used for the assay, being exposed to fluorescent

CS microparticles at 50 and 200 μg/cm^2. Microparticles were aerosolised using a Dry Powder Insufflator™ (Model DP-4, Penn-Century™, USA) and cell samples prepared as described elsewhere [7]. Untreated cells were considered the negative control. For each dose, experiments were performed at least three times ($n \geq 3$).

Macrophage-differentiated THP-1 cells (3.5 x 10^5 cells/well) were further incubated (24 h) with drug-loaded CS microparticles and CS polymer (raw material) to evaluate the induction of TNF-α and IL-8 secretion. Cell supernatants (100 μL) were centrifuged (16,000 *xg*, 5 min) and the cytokines quantified using ELISA kits. Absorbance was detected at 450 nm with background correction at 540 nm. Values were expressed according to reference standard curves. The level of cytokines obtained from LPS- and CCM-treated cells were used as control.

2.9. In vitro antibacterial effect

The susceptibility of *Mycobacterium bovis* BCG (DSM 43990; a gift from Universidade Nova de Lisboa – CEDOC/FCM-UNL) was evaluated *in vitro*. The minimum concentration of drug-loaded CS microparticles required to inhibit mycobacteria growth by 95–100% was determined by the MTT assay, according to a previously described protocol [5].

Assays were conducted after bacterial suspensions achieved an optical density value (OD_{600nm}) of approximately 0.2, as measured by spectrophotometry (Infinite M200, Tecan, Austria). Bacterial suspensions (20 μL, n = 3) were inoculated with test samples serially diluted (180 μL). Bacterial suspension inoculated with broth in the absence of test samples were assumed as positive control, whereas M7H9 medium only (200 μL) was considered as negative control. Free drugs were also tested as control. After 1-week incubation (37 °C, Binder, USA), MTT (30 μL) sterile solution was added, following 1 h

incubation before the addition of DMSO (50 µL). Measurements (n = 3) were conducted by spectrophotometry at 540 nm.

2.10. Statistical analysis

Sigmaplot (version 12.5) was used to statistically analyse the generated data. Student t-test and one-way analysis of variance (ANOVA) with the pairwise multiple comparison procedures (Holm-Sidak method) were performed. Differences were considered significant when *p*-values were smaller than 0.05.

3. Results and Discussion

3.1. Production and characterisation of chitosan microparticles

Spray-drying yielded 75 ± 5% of dry powder, which is satisfactory and actually higher than other values recently reported for spray-dried CS microparticles [6,11]. In this case, high yields could be mainly attributed to the instrumentation design, since the use of high performance cyclone, instead of the manufacturer's standard separator, greatly improved the powder yield [12]. The simultaneous association of INH and RFB to CS microparticles was effective, complying with the combined therapeutic regimen of TB, recommended by WHO [1]. Microparticles presented high and similar association efficiencies – INH (93 ± 4%) and RFB (99 ± 5%) – despite the different aqueous solubilities: 125 mg/mL for INH [7] and 0.19 mg/mL for RFB [13]. Loading capacity of both antibiotics was found to be 8.1 ± 0.3% (INH) and 4.3 ± 0.2% (RFB), values close to the theoretical maximum (8.7% for INH and 4.4% for RFB). In this work, INH was included in higher amount than RFB, as the latter is a more potent antibiotic [14], and also has a more toxic profile, as demonstrated later (section 3.4). Moreover, the amount

of CS in microparticles was maintained purposely high in order to favour macrophage internalisation [3].

These results demonstrate the great capacity of spray-drying to provide drug association, similarly to what was reported for other CS-based microparticles associating antitubercular drugs. However, unlike the present study, the production of the referred microparticles required more than one production step and involved the use of a crosslinking agent (e.g. tripolyphosphate) in order to improve drug retention in the formulation [6]. The literature reports the production of CS microparticles loaded with one [6,15] or more antitubercular drugs [16], using spray-drying or other methods. Nevertheless, such studies included dispersing agents (e.g. lactose) and/or other polysaccharides (e.g. alginate) in the process. To the best of our knowledge, this is the first report describing single step produced spray-dried CS microparticles, combining INH and RFB in a single formulation.

The morphological analysis showed that CS microparticles are spherical, with wrinkled surfaces that generally become smoother after drug incorporation (Figure 1). These morphologies are coincident with previous descriptions of spray-dried CS microparticles [17]. The median volume diameter ($D_{(v,0.5)}$) was determined as 5.9 ± 1.7 µm for drug-loaded microparticles, which agrees with Figure 1.

Insert [Figure 1 near here]

The aerosolisation properties of CS microparticles were investigated *in vitro* using an ACI and the obtained data are displayed in Table 1. The assessment revealed high emitted doses (80–90%) with respirable fractions (FPF ≤ 5µm) of approximately 45%, indicating adequate flowability of microparticles, and supporting the intended

application. Moreover, drug recoveries were found to be 91 ± 4% (INH) and 87 ± 1% (RFB), complying with the recommendations of the European Pharmacopeia [9].

Insert [Table 1 near here]

The formulation generated adequate aerosol size (MMAD around 4 μm) for efficient lung deposition, as particles with aerodynamic diameter of 1-5 μm have great tendency to reach the respiratory zone, while those with less than 2 μm are prone to deposit in peripheral airways [18]. Therefore, drug-loaded CS microparticles display suitable aerodynamic diameter to reach the respiratory zone and possibly to be internalised by macrophages, the target cells, which are described to uptake particulate material with diameter within 1–6 μm [19].

Drug deposition profiles evidenced co-deposition of both INH and RFB on the different ACI stages (Figure 2). This observation reinforces that spray-drying was adequate to associate two antibiotics in a single dry powder formulation for an application in TB therapy, as the drugs are evenly distributed. In summary, the proposed systems exhibited acceptable aerodynamic properties for deep lung delivery of anti-TB drugs.

Insert [Figure 2 near here]

3.2. *Drug release profiles*

Drug release profiles were determined in PBS pH 7.4, containing 1% (v/v) Tween 80®, which mimics the natural surfactant existent in the lung lining fluid [20], and also facilitates RFB dissolution in the medium, considering its poor water solubility. The

release of drugs was further assessed in a medium of pH 5 that simulates the intracellular environment of alveolar macrophages [21].

Figure 3 shows the release of INH and RFB from CS microparticles. The two antibiotics evidenced complete release within two hours (Figure 3 a,b). At pH 7.4 and at initial time points, the release of RFB was slower compared to INH (Figure 3 a, $p < 0.05$). At these time points, the amount of RFB was below the limit of detection, justifying plotting only from 30 min on, time at which about 70% of RFB was released. On the other hand, INH released almost completely (over 90%) in the same period and RFB reached approximately 100% release at 120 min. However, in acidic medium, no significant difference was perceived between INH and RFB profiles at any time point (Figure 3 b). Although not statistically significant, RFB showed faster release at pH 5 (97% at 60 min) than at pH 7.4 (87% at 60 min), certainly due to its higher solubility in acidic medium. Overall, drug release profiles exhibited similar patterns in both media, suggesting that pH does not have a significant impact on drug release from CS microparticles.

Insert [Figure 3 near here]

The release of both drugs under both conditions was similar to that reported for other polysaccharide microparticles loaded with either INH [23] or RFB proposed for pulmonary delivery [24]. Although not immediate, the release may be considered rapid, as in all cases over 70% of the drug was released in the first 30 min. Nevertheless, it must be considered that the used *in vitro* setting does not represent accurately the lung physiology. In fact, the amount of liquid is overestimated in the assay, as microparticles are immersed in the release media, not simulating the volume and thickness of alveolar lung lining fluid [25]. In this way, the rapid release of the drugs, which follows

microparticle dissolution, is certainly different from *in vivo* environment, wherein microparticles would be only partially in contact with the alveolar fluid. Thus, *in vivo* profiles will probably show slower release of drugs [25,26].

3.3. Evaluation of cytotoxicity

The effect of unloaded and drug-loaded CS microparticles on cell viability was evaluated in A549 cells and macrophage-differentiated cells by the MTT assay. For the purpose of discussion, the occurrence of a cytotoxic effect was assumed when the material decreased cell viability below 70% [27].

The exposure of A549 cells to drug-loaded CS microparticles revealed cell viability over 70% at all tested concentrations and at both time points (3 h and 24 h), as depicted in Figure 4 a,b. These results indicate absence of cytotoxicity of the formulation. However, despite no significant differences were observed in terms of dose, the viability of A549 cells decreased over time, suggesting a time-dependent effect ($p<0.05$). In turn, a dose-dependent effect was perceived on macrophage-differentiated THP-1 cells, as cell viability decreased from 90% (0.1 mg/mL) to 59% at the highest tested dose (1.0 mg/mL) upon 24 h exposure ($p<0.05$, Figure 4 b). The observed toxic effect of microparticles on these cells is possibly related with RFB content, an antibiotic that has also shown to be toxic *in vivo* [28]. Overall, both cell lines tolerated well the exposure to unloaded CS microparticles (Figure 4 a,b), which is in agreement with other studies showing low toxicity of CS-based systems tested in the same cell lines [29,30]. The effect of the free drugs, in the concentrations corresponding to those loaded in the microparticles, was reported in a previous work [5]. Free INH showed mild effect on the viability of both cell lines, remaining above 76% in all tested conditions. Oppositely, free RFB (0.05 mg/mL, the highest concentration tested) induced around 50% cell viability in the two cell lines.

A concentration-dependent effect of RFB on cell viability was confirmed in the present work by testing microparticles with lower RFB content (CS/INH/RFB = 10/1/0.2, w/w), which were purposely produced to undergo this assay. The decrease in RFB loading led to viability of macrophage-like cells above 70% in all tested conditions referred above (data not shown). Interestingly, free RFB at 0.025 mg/mL had demonstrated a cytotoxic effect 24 h-post exposure to macrophage-differentiated THP-1 cells [5], but the detrimental effect was not perceived for drug-loaded CS microparticles at the same time point (Figure 4 b). Therefore, it is suggested that microencapsulation may revert RFB cytotoxic effect at some extent ($p<0.05$), as proposed previously [5].

Insert [Figure 4 near here]

It must be mentioned that the highest dose tested in the present study is considered much higher than that to be observed *in vivo* upon inhalation, taking into account the large area of the alveolar zone [31]. Therefore, *in vivo* concentrations will most likely correlate those of the lower doses tested, at which no cytotoxicity were perceived. In this sense, both cell lines were considered to tolerate well the exposure to CS/INH/RFB microparticles.

Complementarily to the determination of cell viability through metabolic activity, the cell membrane integrity was assessed by determining the level of LDH released from both cell lines upon exposure to the microparticles and free drugs.

The incubation with CCM resulted in basal release of LDH of 21% and 34%, for A549 and macrophage-differentiated THP-1 cells, respectively (Figure 5). Unloaded CS microparticles did not raise the release of the enzyme, evidencing that CS itself did not show toxic effect on any cell line (Figure 5), as also reported elsewhere [32,33].

Insert [Figure 5 near here]

Drug-loaded microparticles exhibited toxicity on macrophage-differentiated THP-1 cells, with 49% LDH release, which is higher than the 34% of CCM ($p<0.05$). Unexpectedly, A549 cells also showed significantly increased release of LDH (28%) upon exposure to drug-loaded microparticles, compared with CCM ($p<0.05$, Figure 5). This slight cytotoxicity was not evident in the MTT assay (cell viability around 80%). Despite the increased release of LDH observed in both cell lines, the developed carriers induced lower LDH release than free RFB ($p<0.05$) and an effect similar to that of free INH, thus suggesting the ability of microencapsulation to potentially reduce drug toxicological effects. Data regarding the exposure of both cell lines to free drugs were presented in a previous publication [5]. Importantly, the level of enzyme secreted after exposure to microparticles is far lower than the observed for the positive control.

The different outcomes registered in both assays (MTT and LDH release) have been reported [34] and are due to the fact that the two methods assess cell-particle interactions in different ways. Microparticles possibly interact with cytoplasmic membrane, promoting cell lysis, but not necessarily interfere with intracellular functions, such as mitochondrial dehydrogenase activity [35]. Contrarily, particles may enhance metabolic activity, despite the small number of viable cells, leading to an overestimation of cell viability, determined by MTT assay [36]. Therefore, the measurement of LDH release should be taken as a complement to the MTT assay, but there is the need to extend the range of tests to rigorously characterise the safety profile of the proposed carriers.

3.4. Interaction of microparticles with macrophages

Considering the intended application of the produced carriers, both the phagocytosis of microparticles and the subsequent induction of macrophage activation would be beneficial. The preliminary internalisation of CS microparticles was assessed in macrophage-differentiated THP-1 cells and rat alveolar macrophages NR8383. Cells were exposed to fluorescently-labelled CS microparticles for 2 h, since 50 – 75% of microparticles are reported to be phagocytosed within 2–3 h [37]. Microparticle uptake by differentiated THP-1 cells was very high at both concentrations (94.3 ± 1.5 for 50 µg/cm^2 and 98.1 ± 1.8% for 200 µg/cm^2), as depicted in Figure 6. Likewise, NR8383 cells internalised up to 99.9 ± 0.1, regardless of the dose. These preliminary results suggest high affinity of macrophages for CS microparticles independently of concentrations and cell type. It is well-known that macrophages are specialised cells, which recognise and engulf particulate matter, and thus the internalisation of particles was expected. Nevertheless, residues of *N*-acetylglucosamine, a structural unit of CS, have been described to be preferentially recognised by macrophages [3]. The presence of such units possibly mediated the phagocytic mechanism, which could explain the high affinity of cells for the produced microparticles. However, it is deemed adequate to consider future assays providing comparison with a material devoid of units recognised by macrophages. In this way, the favourable recognition of CS-based carriers by macrophage-like cells could be unequivocally established. Furthermore, complementation with confocal microscopy would strenghten the data.

Insert [Figure 6 near here]

Following phagocytosis, macrophages may become activated, which contributes to the efficient control of the proliferation and dissemination of pathogens by producing

cytokines (e.g. TNF-α and IL-8) [38]. Such pro-inflammatory cytokines are reported to be secreted by human alveolar macrophages upon infection with *M. tuberculosis* [39]. In light of this, macrophage-differentiated THP-1 cells were exposed (24 h) to CS/INH/RFB microparticles and the levels of TNF-α and IL-8 were quantitatively determined in cell culture supernatants. CCM and lipopolysaccharide (LPS) were used as negative and positive controls, respectively [5].

Drug-loaded microparticles induced the secretion of a considerable amount of cytokines, 614 pg/mL for TNF-α and 10.6 x 10^3 pg/mL for IL-8 (Figure 7 a,b). In both cases the values were much higher compared with basal secretion of cells incubated with CCM ($p<0.05$). No significant differences were found between TNF-α secretion promoted by loaded carriers and CS polymer (Figure 7 a), but a significant difference was observed for IL-8 (Figure 7 b; $p<0.05$). In that case, drug association apparently interfered with cell receptor signaling during immune activation, thus decreasing macrophage activation ability. A possible explanation for this effect is that the lenght of the released polymeric chain and also the number of fractions of *N*-acetylglucosamine residues influence the level of immune activation, and drug association can possibly alter this pattern [40]. As referred previously, *N*-acetylglucosamine moieties have reported recognition by macrophage receptors [3], thus, possibly, inducing cell activation.

Although the formulation induced cytokine production at lower levels compared to LPS, the exposure of macrophage-like cells to CS microparticles resulted in the increased release of TNF-α and IL-8 in relation to CCM ($p<0.05$). Other studies describe similar effects [6,41]. Although the natural immunomodulatory properties of CS have been already demonstrated [42], the mechanism through which CS particles induce immune response still needs to be unveiled.

Insert [Figure 7 near here]

3.5. In vitro antibacterial effect

The viability of *M. bovis* DSM 43990 cells was verified upon exposure to drug-loaded CS microparticles and free drugs (either alone or in combination). MIC values were calculated in relation to control (culture of mycobacteria), assumed as 100% bacterial growth. MIC value of free INH was 0.125 µg/mL, being alligned with literature descriptions [43]. RFB had a much lower MIC value (0.004 µg/mL), evidencing its higher antimicrobial effect compared to INH. This is possibily related to RFB lipophilicity, which may facilitate cell membrane permeation [44]. Different MIC values of RFB have been reported, varying according to the methodologies used to test suceptibility and the tested strains of *M. bovis* [43].

In combination, free INH and RFB inhibited bacterial growth by 94 ± 1%, presenting MIC values of 0.008 µg/mL and 0.004 µg/mL, respectively. Curiously, the MIC of INH alone (0.125 µg/mL) decreased in the presence of RFB, which MIC remained unchanged. This different behaviour between INH and other antibiotics has been described [45] and the stronger antibacterial acitivity of RFB compared to INH is also reported [14]. Additionally, a dose of 0.08 µg/mL of drug-loaded CS microparticles was the minimum concentration needed to inhibit mycobacterial growth by 96 ± 1%. At this concentration, microparticle drug contents are approximately 0.007 µg/mL (INH) and 0.004 µg/mL (RFB), considering the association efficiencies. It is worth noting that these results are in line with MIC values determined for the combined solution of free antibiotics. In other words, no differences were perceived in terms of inhibition effects comparing drug-loaded CS microparticles (96 ± 1%) and free INH/RFB (94 ± 1%). This indicates that the combined microencapsulation of the drugs did not intefere with their

antibacterial activity. As well, results demonstrate that the proposed formulation can potentially inhibit the growth of *M. bovis in vitro*.

Conclusion

Inhalable CS dry powder loaded with both INH and RFB was prepared by spray-drying, with drug association efficiencies of 93% (INH) and 99% (RFB). The developed microparticles displayed MMAD around 4 µm and FPF of approximately 45%, thus showing suitable aerodynamic properties for deep lung delivery. Cytotoxicity assays demonstrated that the formulation is well tolerated by alveolar epithelial cells. Nevertheless, a slight decrease on cell viability of macrophage-like cells (to 60%) was observed at the highest microparticle concentration tested (1.0 mg/mL) after 24 h exposure, although this dose is possibly overestimated comparing to real *in vivo* conditions. Furthermore, a preliminary evaluation indicated strong ability of CS microparticles to undergo macrophage uptake *(*up to 99.9%) and the ability to induce macrophage activation. Additionally, drug antibacterial activity against *M. bovis* was demonstrated to be preserved after drug microencapsulation. In conclusion, the developed dual drug-loaded CS microparticles demonstrated to be potential candidates for inhalable therapy of pulmonary TB. Despite that, long-term effects of CS microparticles upon pulmonary administration *in vivo*, along with *in vivo* antibacterial efficacy of the systems, are very relevant evaluations to perform in the future.

Declaration of interest statement

The authors declare no conflict of interest.

Acknowledgements

Funding from the Portuguese Foundation for Science and Technology (PTDC/DTP-FTO/0094/2012, UID/Multi/04326/2013 and UID/BIM/04773/2013) is acknowledged. Ludmylla Cunha acknowledges PhD grant (BEX 1168/13-4) supported by CAPES – Brazil.

References

1. World Health Organization *Global Tuberculosis Report 2017. World Health Organization, Geneva.*; Geneva, Switzerland, 2017;
2. Liang, Z.; Ni, R.; Zhou, J.; Mao, S. Recent advances in controlled pulmonary drug delivery. *Drug Discov. Today* **2015**, *20*, 380–389, doi:10.1016/j.drudis.2014.09.020.
3. East, L.; Isacke, C. M. The mannose receptor family. *Biochim. Biophys. Acta - Gen. Subj.* **2002**, *1572*, 364–386.
4. Cunha, L.; Rosa da Costa, A. M.; Lourenço, J. P.; Buttini, F.; Grenha, A. Spray-dried fucoidan microparticles for pulmonary delivery of antitubercular drugs. *J. Microencapsul.* **2018**, *35*, 392–405, doi:10.1080/02652048.2018.1513089.
5. Cunha, L.; Rodrigues, S.; Buttini, F.; Grenha, A. Inhalable fucoidan microparticles combining two antitubercular drugs with potential application in pulmonary tuberculosis therapy. *Polymers (Basel).* **2018**, *10*, 1–19, doi:10.3390/polym10060636.
6. Oliveira, P. M.; Matos, B. N.; Pereira, P. A. T.; Gratieri, T.; Faccioli, L. H.; Cunha-Filho, M. S. S.; Gelfuso, G. M. Microparticles prepared with 50–190 kDa chitosan as promising non-toxic carriers for pulmonary delivery of isoniazid. *Carbohydr. Polym.* **2017**, *174*, 421–431, doi:10.1016/J.CARBPOL.2017.06.090.
7. Alves, A.; Cavaco, J.; Guerreiro, F.; Lourenço, J.; Rosa da Costa, A.; Grenha, A. Inhalable antitubercular therapy mediated by locust bean gum microparticles.

Molecules **2016**, *21*, 1–22, doi:10.3390/molecules21060702.

8. Martinelli, F.; Balducci, A. G.; Kumar, A.; Sonvico, F.; Forbes, B.; Bettini, R.; Buttini, F. Engineered sodium hyaluronate respirable dry powders for pulmonary drug delivery. *Int. J. Pharm.* **2017**, *517*, 286–295, doi:10.1016/j.ijpharm.2016.12.002.

9. Buttini, F.; Colombo, G.; Kwok, P. C. L.; Wui, W. T. Aerodynamic assessment for inhalation products: Fundamentals and current pharmacopoeial methods. In *Inhalation drug delivery: Techniques and products*; Colombo, P. Traini, D. and Buttini, F., Ed.; Wiley-Blackwell: West Sussex, United Kingdom, 2013; pp. 91–119.

10. Lund, M. E.; To, J.; O'Brien, B. A.; Donnelly, S. The choice of phorbol 12-myristate 13-acetate differentiation protocol influences the response of THP-1 macrophages to a pro-inflammatory stimulus. *J. Immunol. Methods* **2016**, *430*, 64–70, doi:10.1016/j.jim.2016.01.012.

11. Pai, R. V.; Jain, R. R.; Bannalikar, A. S.; Menon, M. D. Development and evaluation of chitosan microparticles based dry powder inhalation formulations of rifampicin and rifabutin. *J. Aerosol Med. Pulm. Drug Deliv.* **2015**, *28*, 1–17, doi:10.1089/jamp.2014.1187.

12. Maury, M.; Murphy, K.; Kumar, S.; Shi, L.; Lee, G. Effects of process variables on the powder yield of spray-dried trehalose on a laboratory spray-dryer. *Eur. J. Pharm. Biopharm.* **2005**, *59*, 565–573.

13. Anshakova, A. V; Yu Konyukhov, V. Study by inverse gas chromatography of the solubility of rifabutin in water in the presence of cyclodextrin. *Russ. J. Appl. Chem.* **2017**, *90*, 209–213, doi:10.1134/S1070427217020082.

14. Jabes, D.; Della Bruna, C.; Rossi, R.; Olliaro, P. Effectiveness of rifabutin alone

or in combination with isoniazid in preventive therapy of mouse tuberculosis. *Antimicrob. Agents Chemother.* **1994**, *38*, 2346–2350, doi:10.1128/AAC.38.10.2346.

15. Lacerda, L.; Parize, A. L.; Fávere, V.; Laranjeira, M. C. M.; Stulzer, H. K. Development and evaluation of pH-sensitive sodium alginate/chitosan microparticles containing the antituberculosis drug rifampicin. *Mater. Sci. Eng. C* **2014**, *39*, 161–167, doi:10.1016/J.MSEC.2014.01.054.

16. Pandey, R.; Khuller, G. K. Chemotherapeutic potential of alginate-chitosan microspheres as anti-tubercular drug carriers. *J. Antimicrob. Chemother.* **2004**, *53*, 635–640, doi:10.1093/jac/dkh139.

17. Corrigan, D. O.; Healy, A. M.; Corrigan, O. I. Preparation and release of salbutamol from chitosan and chitosan co-spray dried compacts and multiparticulates. *Eur. J. Pharm. Biopharm.* **2006**, *62*, 295–305.

18. Buttini, F.; Brambilla, G.; Copelli, D.; Sisti, V.; Balducci, A. G.; Bettini, R.; Pasquali, I. Effect of flow rate on in vitro aerodynamic performance of NEXThaler ® in comparison with Diskus ® and Turbohaler ® Dry Powder Inhalers. *J. Aerosol Med. Pulm. Drug Deliv.* **2016**, *29*, 167–178, doi:10.1089/jamp.2015.

19. Hirota, K.; Hasegawa, T.; Hinata, H.; Ito, F.; Inagawa, H.; Kochi, C.; Soma, G. I.; Makino, K.; Terada, H. Optimum conditions for efficient phagocytosis of rifampicin-loaded PLGA microspheres by alveolar macrophages. *J. Control. Release* **2007**, *119*, 69–76, doi:10.1016/j.jconrel.2007.01.013.

20. Eleftheriadis, G. K.; Akrivou, M.; Bouropoulos, N.; Tsibouklis, J.; Vizirianakis, I. S.; Fatouros, D. G. Polymer−lipid microparticles for pulmonary delivery. *Langmuir* **2018**, *34*, 3438–3448, doi:10.1021/acs.langmuir.7b03645.

21. Vieira, A. C.; Magalhães, J.; Rocha, S.; Cardoso, M. S.; Santos, S. G.; Borges, M.; Pinheiro, M.; Reis, S. Targeted macrophages delivery of rifampicin-loaded lipid nanoparticles to improve tuberculosis treatment. *Nanomedicine* **2017**, *12*, 2721–2736, doi:10.2217/nnm-2017-0248.

22. Chauhan, D.; Patel, A.; Shah, S. Influence of selected natural polymers on in-vitro release of colon targeted Mebeverine HCl matrix tablet. *Int. J. Drug Dev. Res.* **2012**, *4*, 247–255.

23. Kundawala, A. J.; Patel, V. a; Patel, H. V; Choudhary, D. Influence of formulation components on aerosolization properties of isoniazid loaded chitosan microspheres. *Intenational J. Pharm. Sci. Drug Res.* **2011**, *3*, 297–302.

24. Upadhyay, T. K.; Fatima, N.; Sharma, D.; Saravanakumar, V.; Sharma, R. Preparation and characterization of beta-glucan particles containing a payload of nanoembedded rifabutin for enhanced targeted delivery to macrophages. *EXCLI J.* **2017**, *16*, 210–228, doi:10.17179/excli2016-804.

25. Haghi, M.; Ong, H. X.; Traini, D.; Young, P. Across the pulmonary epithelial barrier: Integration of physicochemical properties and human cell models to study pulmonary drug formulations. *Pharmacol. Ther.* **2014**, *144*, 235–252, doi:10.1016/J.PHARMTHERA.2014.05.003.

26. Bur, M.; Huwer, H.; Muys, L.; Lehr, C.-M. Drug transport across pulmonary epithelial cell monolayers: Effects of particle size, apical liquid volume, and deposition technique. *J. Aerosol Med. Pulm. Drug Deliv.* **2010**, *23*, 119–127, doi:10.1089/jamp.2009.0757.

27. ISO 10993-5 *Biological Evaluation of Medical Devices Part 5: Tests for In Vitro Cytotoxicity. International Organization for Standardization.*; Geneva, Switzerland, 2009;

28. Barluenga, J.; Aznar, F.; García, A. B.; Cabal, M. P.; Palacios, J. J.; Menéndez, M. A. New rifabutin analogs: Synthesis and biological activity against Mycobacterium tuberculosis. *Bioorganic Med. Chem. Lett.* **2006**, *16*, 5717–5722, doi:10.1016/j.bmcl.2006.08.090.

29. Abbas, Y.; Azzazy, H. M. E.; Tammam, S.; Lamprecht, A.; Ali, M. E.; Schmidt, A.; Sollazzo, S.; Mathur, S. Development of an inhalable, stimuli-responsive particulate system for delivery to deep lung tissue. *Colloids Surfaces B Biointerfaces* **2016**, *146*, 19–30, doi:10.1016/J.COLSURFB.2016.05.031.

30. Boyles, M. S. P.; Kristl, T.; Andosch, A.; Zimmermann, M.; Tran, N.; Casals, E.; Himly, M.; Puntes, V.; Huber, C. G.; Lütz-meindl, U.; Duschl, A. Chitosan functionalisation of gold nanoparticles encourages particle uptake and induces cytotoxicity and pro-inflammatory conditions in phagocytic cells, as well as enhancing particle interactions with serum components. *J. Nanobiotechnology* **2015**, *13*, 1–20, doi:10.1186/s12951-015-0146-9.

31. Fröhlich, E.; Mercuri, A.; Wu, S.; Salar-Behzadi, S. Measurements of deposition, lung surface area and lung fluid for simulation of inhaled compounds. *Front. Pharmacol.* **2016**, *7*, 1–10, doi:10.3389/fphar.2016.00181.

32. Caetano, L. A.; Almeida, A. J.; Gonçalves, L. M. D. Effect of experimental parameters on alginate / chitosan microparticles for BCG encapsulation. *Mar. Drugs* **2016**, *14*, 1–30, doi:10.3390/md14050090.

33. Fu, Y. N.; Li, Y.; Li, G.; Yang, L.; Yuan, Q.; Tao, L.; Wang, X. Adaptive Chitosan Hollow Microspheres as Efficient Drug Carrier. *Biomacromolecules* **2017**, *18*, 2195–2204, doi:10.1021/acs.biomac.7b00592.

34. Fotakis, G.; Timbrell, J. A. In vitro cytotoxicity assays: Comparison of LDH, neutral red, MTT and protein assay in hepatoma cell lines following exposure to

cadmium chloride. *Toxicol. Lett.* **2006**, *160*, 171–177, doi:10.1016/j.toxlet.2005.07.001.

35. Wang, C.; Muttil, P.; Lu, D.; Beltran-Torres, A. A.; Garcia-Contreras, L.; Hickey, A. J. Screening for potential adjuvants administered by the pulmonary route for tuberculosis vaccines. *AAPS J.* **2009**, *11*, 139–147, doi:10.1208/s12248-009-9089-0.

36. Braz, L.; Grenha, A.; Ferreira, D.; Rosa da Costa, A. M. A. M.; Gamazo, C.; Sarmento, B. Chitosan/sulfated locust bean gum nanoparticles: In vitro and in vivo evaluation towards an application in oral immunization. *Int. J. Biol. Macromol.* **2017**, *96*, 786–797, doi:10.1016/j.ijbiomac.2016.12.076.

37. Geiser, M. Update on macrophage clearance of inhaled micro- and nanoparticles. *J. Aerosol Med. Pulm. Drug Deliv.* **2010**, *23*, 207–217.

38. Fujihara, M.; Muroi, M.; Tanamoto, K.; Suzuki, T. Molecular mechanisms of macrophage activation and deactivation by lipopolysaccharide: Roles of the receptor complex. *Pharmacol. Ther.* **2003**, *100*, 171–194, doi:10.1016/j.pharmthera.2003.08.003.

39. JoAnne L. Flynn and John Chan Immunology of tuberculosis. *Annu. Rev. Immunol.* **2001**, *19*, 93–129, doi:10.4084/MJHID.2014.027.

40. Brodaczewska, K.; Wolaniuk, N.; Lewandowska, K.; Donskow-Łysoniewska, K.; Doligalska, M. Biodegradable chitosan decreases the immune response to Trichinella spiralis in mice. *Molecules* **2017**, *22*, 1–16, doi:10.3390/molecules22112008.

41. Caires, H. R.; Esteves, T.; Quelhas, P.; Barbosa, M. A.; Navarro, M.; Almeida, C. R. Macrophage interactions with polylactic acid and chitosan scaffolds lead to improved recruitment of human mesenchymal stem/stromal cells: A

comprehensive study with different immune cells. *J. R. Soc. Interface* **2016**, *13*, 1–12, doi:10.1098/rsif.2016.0570.

42. Singh, B.; Maharjan, S.; Cho, K.-H.; Cui, L.; Park, I.-K.; Choi, Y.-J.; Cho, C.-S. Chitosan-based particulate systems for the delivery of mucosal vaccines against infectious diseases. *Int. J. Biol. Macromol.* **2018**, *110*, 54–64, doi:10.1016/J.IJBIOMAC.2017.10.101.

43. Ritz, N.; Tebruegge, M.; Connell, T. G.; Sievers, A.; Robins-Browne, R.; Curtis, N. Susceptibility of Mycobacterium bovis BCG vaccine strains to antituberculous antibiotics. *Antimicrob. Agents Chemother.* **2009**, *53*, 316–318, doi:10.1128/AAC.01302-08.

44. Feng, H.; Zhang, L.; Zhu, C. Genipin crosslinked ethyl cellulose-chitosan complex microspheres for anti-tuberculosis delivery. *Colloids Surfaces B Biointerfaces* **2013**, *103*, 530–537, doi:10.1016/j.colsurfb.2012.11.007.

45. Almeida, D.; Nuermberger, E.; Tasneen, R.; Rosenthal, I.; Tyagi, S.; Williams, K.; Peloquin, C.; Grosset, J. Paradoxical effect of isoniazid on the activity of rifampin-pyrazinamide combination in a mouse model of tuberculosis. *Antimicrob. Agents Chemother.* **2009**, *53*, 4178–4184, doi:10.1128/AAC.00830-09.

Figure captions

Figure 1. Scanning electron microphotographs of (a) unloaded chitosan microparticles and (b) chitosan microparticles loaded with isoniazid and rifabutin.

Figure 2. Aerodynamic deposition profiles (n = 3, mean ± SD) of isoniazid (INH) and rifabutin (RFB) in the Andersen Cascade Impactor. Drugs were associated with spray-dried chitosan microparticles. Cps: capsule; Dev.: inhaler device; F: filter; IP: induction port; St: stage.

Figure 3. *In vitro* release of isoniazid (INH) and rifabutin (RFB) from chitosan microparticles in (a) PBS pH 7.4-Tween 80® and b) buffer at pH 5.0-Tween 80®. Mean ± SD (n = 3). *p<0.05 comparing release of the two drugs.

Figure 4. Viability of A549 (lighter colours) and macrophage-differentiated THP-1 cells (darker colours) upon a) 3 h and b) 24 h exposure to unloaded and drug-loaded chitosan (CS) microparticles (CS/INH/RFB = 10/1/0.5, w/w). Data are expressed as a percentage of untreated cells (positive control) and indicate mean ± SEM (n = 3, six replicates per experiment at each concentration). Dashed lines represent 70% cell viability.

Figure 5. Percentage of LDH released from A549 cells (lighter colours) and macrophage-differentiated THP-1 cells (darker colours) exposed (24 h) to chitosan (CS) microparticles (1 mg/mL). Triton X-100 and cell culture medium (CCM) were used as positive and negative controls, respectively (data from [5]). Data represent mean ± SEM (n = 3, six replicates per experiment at each concentration). *p<0.05 compared to respective CCM.

Figure 6. Percentage (mean ± SEM; n ≥ 3) of macrophage-differentiated THP-1 cells and NR8383 phagocytosing fluorescently-labelled chitosan microparticles. Cells were exposed (2 h) to 50 and 200 μg/cm^2 of microparticles.

Figure 7. Release of a) TNF-α and b) IL-8 from macrophage-differentiated THP-1 cells induced by chitosan (raw material) and drug-loaded CS microparticles. Cell culture medium (CCM) and lipopolysaccharide (LPS) were used as negative and positive controls, respectively (data from [5]). *p<0.05 compared to CCM.

Table 1. Aerosolisation properties (n = 3, mean ± SD) of chitosan microparticles associating isoniazid (INH) and rifabutin (RFB). The amount of drug loaded corresponds to 2.8 mg of INH and 1.5 mg of RFB, based on the drug content found in the formulation.

Drug	Metered Dose (mg)	Emitted dose (mg)	MMAD (µm)	FPD <5 µm (mg)	FPF <5µm (%)
INH	2.7 ± 0.2	2.5 ± 0.3	4.2 ± 0.1	1.1 ± 0.2	43.6 ± 4.2
RFB	1.3 ± 0.1	1.2 ± 0.2	4.1 ± 0.2	0.5 ± 0.1	45.2 ± 3.1

FPD: fine particle dose; FPF: fine particle fraction; MMAD: mass median aerodynamic diameter.

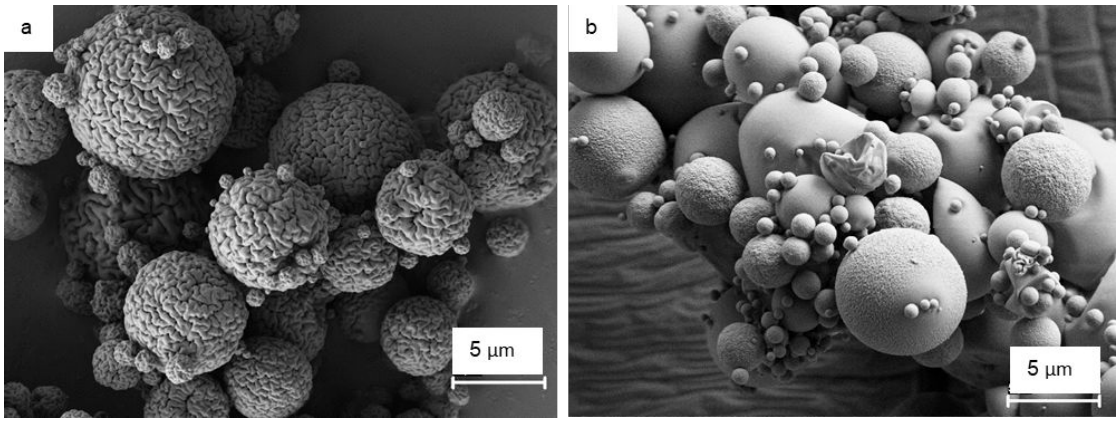

Figure 1

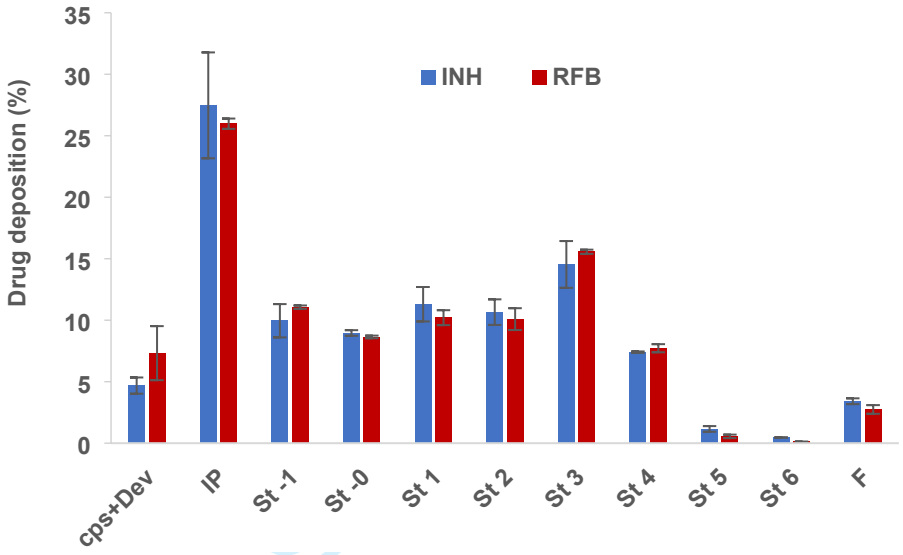

Figure 2

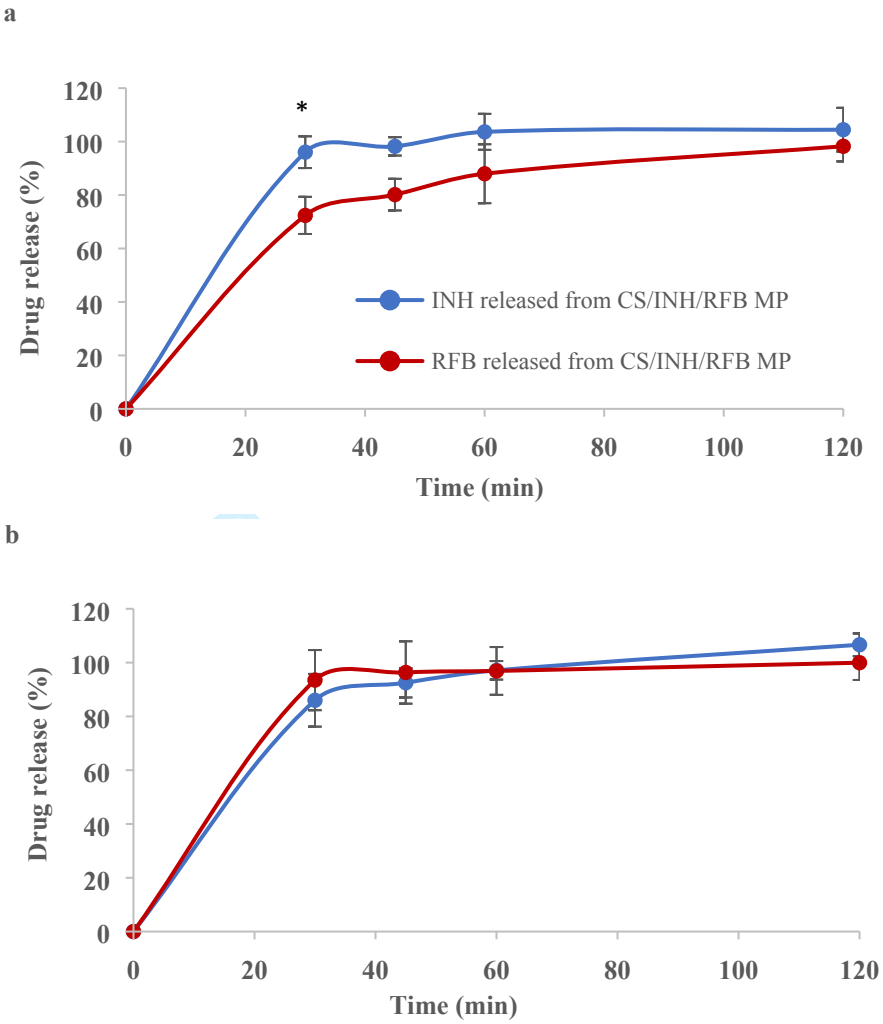

Figure 3

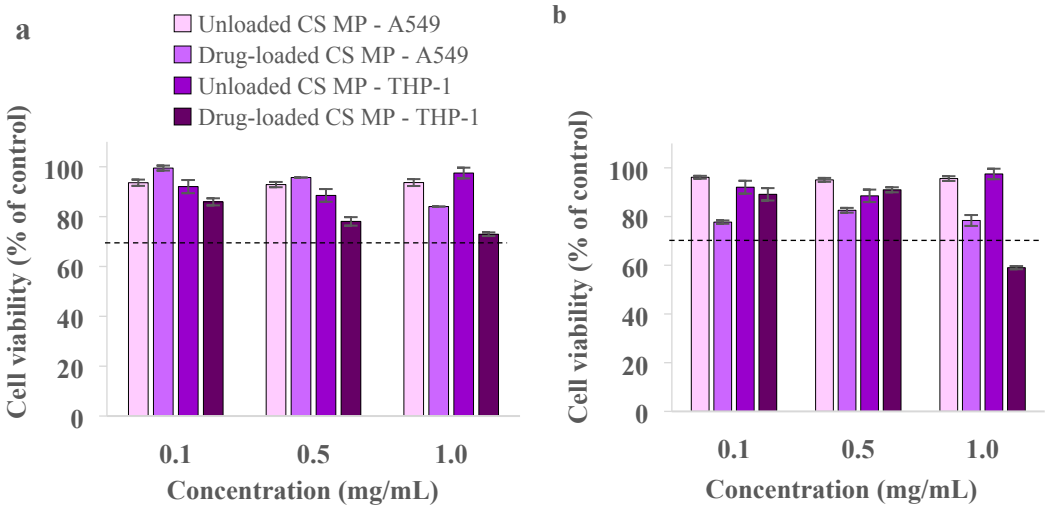

Figure 4

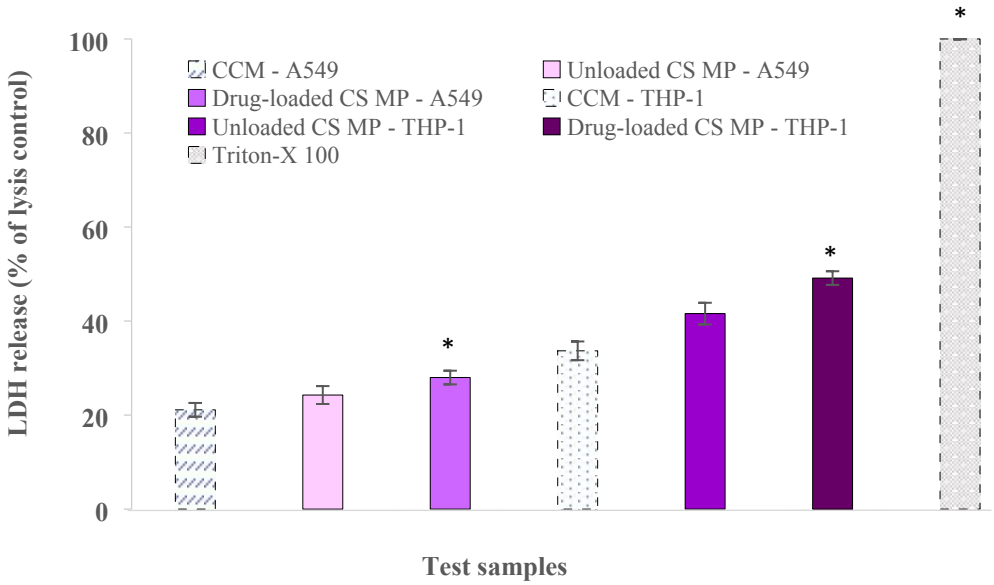

Figure 5

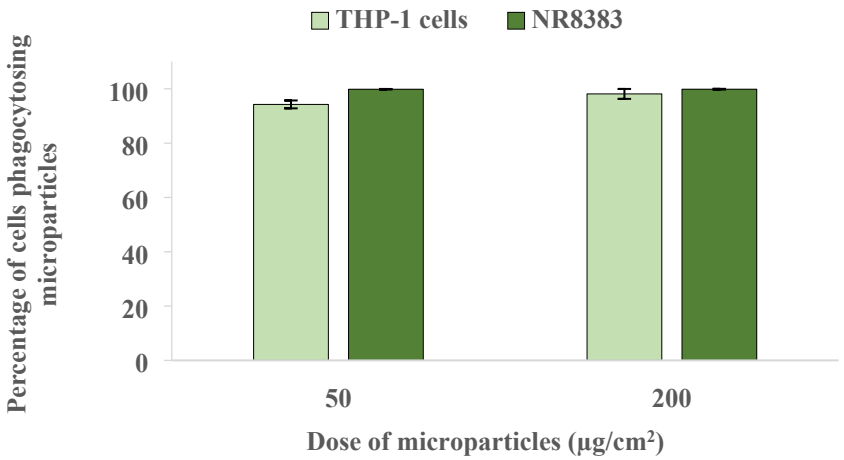

Figure 6

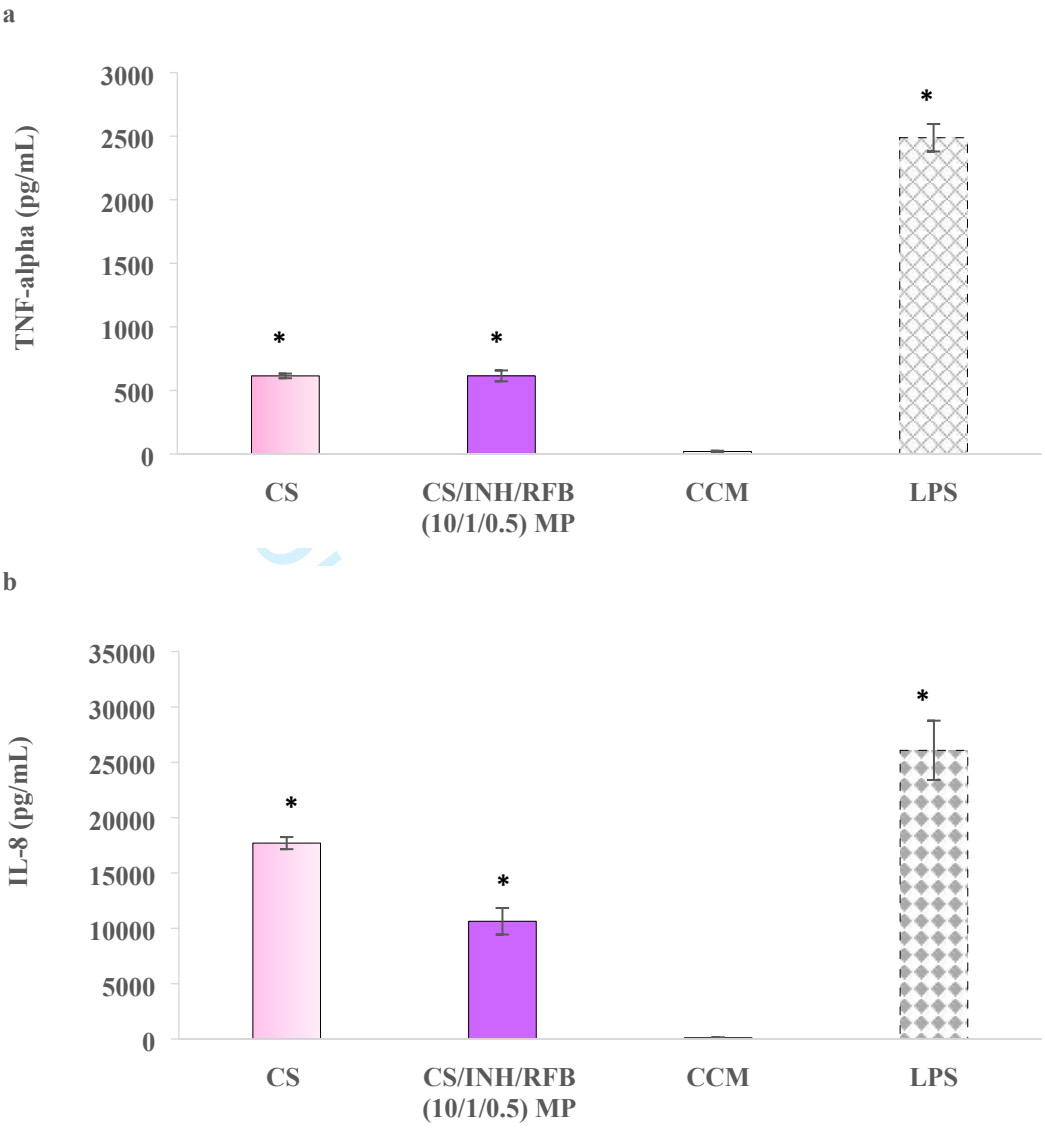
a
TNF-alpha (pg/mL)
3000
2500
2000
1500
1000
500
0
*
*
*
CS
CS/INH/RFB (10/1/0.5) MP
CCM
LPS
b
IL-8 (pg/mL)
35000
30000
25000
20000
15000
10000
5000
0
*
*
*
CS
CS/INH/RFB (10/1/0.5) MP
CCM
LPS

Figure 7